ELSEVIER

Journal of Organometallic Chemistry 635 (2001) 119–131

Journal of Organometallic Chemistry

www.elsevier.com/locate/jorganchem

Reactions of $[Os_3(CO)_{10}(NCMe)_2]$ with symmetric diynes and their reactivity towards $[Co_2(CO)_8]$☆

Angelo J. Amoroso, Lionel P. Clarke, John E. Davies, Jack Lewis, Harold R. Powell, Paul R. Raithby *, Gregory P. Shields

Department of Chemistry, University of Cambridge, Lensfield Road, Cambridge CB2 1EW, UK

Received 3 April 2001; accepted 11 May 2001

Abstract

The reaction between $[Os_3(CO)_{10}(NCMe)_2]$ and MeC_2C_2Me yields the known cluster $[Os_3(CO)_9(\mu\text{-}CO)(\mu_3\text{-}\eta^2\text{-}MeC_2C_2Me)]$ (**1**) and three previously uncharacterised products $[Os_3(CO)_9(\mu\text{-}CO)\{\mu_3\text{-}\eta^2\text{:}\mu_3\text{-}\eta^1\text{:}\eta^1\text{:}\eta^3\text{-}MeC_2C_2MeOC_5Me_2\}Os_3(\mu\text{-}CO)(CO)_9]$ (**2**), $[Os_3(CO)_9\{\mu_3\text{-}\eta^4\text{-}[(MeC_2)C_2(Me)]CO[(Me)C_2(C_2Me)]\}]$ (**3**) and $[Os_3(CO)_9\{\mu_3\text{-}\eta^4\text{-}[(MeC_2)C_2(Me)]CO[(MeC_2)C_2(Me)]\}]$ (**4**). The structures of **2** and **3** have been determined by X-ray crystallography. Cluster **2** incorporates two linked triosmium clusters joined by an unsaturated five-membered metallacycloether ring and **3** exhibits an alkyne-functionalised metallacyclohexadieneone ring. **1**–**4** and $[Os_3(CO)_9(\mu\text{-}CO)(\mu_3\text{-}\eta^2\text{-}PhC_2C_2Ph)]$ (**5**) react with $[Co_2(CO)_8]$ to form products **6**–**11** in which one free alkyne function coordinates to a $Co_2(CO)_6$ unit in each case; the cluster $[\{Os_3(CO)_{10}\}\{Co_2(CO)_6\}\{\mu_3\text{-}\eta^2\text{-}\|\text{-}(MeCC)(\mu_2\text{-}\eta^2(CCMe)\}]$ (**6**) has been structurally characterised. The reaction of **1** and **5** with Me_3NO–MeCN leads to the replacement of one CO ligand with MeCN, the products **12** and **13** reacting with H_2O to form $[Os_3(CO)_9(\mu\text{-}OH)(\mu_3\text{-}\eta^1\text{:}\eta^2\text{:}\eta^2\text{-}RC_3CHR)]$ (R = Me (two isomers **14**, **15**), Ph (**16**)); the X-ray structure of **16** is reported. Reaction of **3** with Me_3NO–MeCN results in the substitution of a CO ligand with either a MeCN or NMe_3 ligand at the metallocyclic Os atom to afford the clusters $[Os_3(CO)_8(L)(\mu_3\text{-}\eta^1\text{:}\eta^1\text{:}\eta^2\text{:}\eta^2\text{-}\{(MeC_2)C_2(Me)\}_2CO)]$ (L = NCMe (**17**), NMe_3 (**18**)).

Keywords: Osmium; Cobalt; Carbonyl clusters; Diyne; X-ray crystal structures

1. Introduction

The chemistry and bonding of alkenes and alkynes coordinated to transition metals is now so well established that it forms a fundamental part of every textbook on organometallic chemistry [1], and our understanding of the bonding in these systems has developed from the original work of Dewar. Similar bonding descriptions may be applied to polynuclear complexes with coordinated alkenes or alkynes, and the chemistry of alkenes and alkynes with trinuclear ruthenium and osmium carbonyl clusters is well documented [2,3]. Alkynes display a wide range of coordination modes and transition-metal mediated carbon–carbon bond formation and cyclisations of unsaturated hydrocarbons are commonplace [4]. Structurally characterised alkyne complexes in which two or more alkynes have cyclised with a molecule of CO to form metallacycloolefinic ketones have also been studied. For example, more than one alkyne molecule may react with the activated clusters $[Os_3(CO)_{10}(NCMe)_2]$ and $[Os_3H_2(CO)_{10}]$ and the incorporation of a CO ligand into the carbon backbone may occur [5,6]. In some cases substituted-alkyne clusters may be treated with one or more equivalents of Me_3NO–MeCN, affording an activated complex, thereby facilitating the incorporation of further alkyne molecules. This can take the form of a regiospecific insertion, thus systematically extending the carbon chain [7].

The related chemistry of 1,3-diynes, where the extended carbon chain is pre-formed, has been less extensively investigated although there is considerable potential for additional modes of coordination between

☆ Special issue dedicated to the 50th Anniversary of Dewar's paper on the bonding in organotransition metal chemistry.

* Corresponding author. Current address: Department of Chemistry, University of Bath, Claverton Down, Bath BA2 7AY, UK. Fax: +44-1225-826231.

E-mail address: p.r.raithby@bath.ac.uk (P.R. Raithby).

0022-328X/01/$ - see front matter
PII: S0022-328X(01)01046-4

the linked multiple bonds and the metal centres [8]. Among the reported investigations are the reactions of the ruthenium clusters $[Ru_3(CO)_{12}]$, $[Ru_3(CO)_{10}(NCMe)_2]$ [9], $[Ru_4(CO)_{13}(\mu_3\text{-PPh})]$ [10], $[Ru_4H_2(CO)_{12}(\mu_3\text{-PPh})]$ [11], $[Ru_4H_4(CO)_{12}]$ [12], and ruthenium-containing mixed-metal systems [13] with selected diynes. Their chemistry displays many similarities with that of the related alkynes, i.e. similar coordination modes are adopted and the organic ligands undergo analogous transformations and cyclisations. In particular, where more forcing conditions are employed, the trinuclear ruthenium systems are characterised by Ru–Ru bond fission and C–C bond formation [9].

In contrast, the trinuclear Os_3 core is more robust and the clusters $[Os_3(CO)_9(\mu\text{-CO})(\mu_3\text{-}\eta^2\text{-}RC_2C_2R')]$ {R = R′ = Ph, ^{t}Bu, $SiMe_3$; R = Ph, R′ = $SiMe_3$}, derived from the reaction of $[Os_3(CO)_{10}(NCMe)_2]$ with the respective diynes [14,15], undergo C–C cleavage to produce the *bis*(alkynyl) clusters $[Os_3(CO)_9(\mu_3\text{-}\eta^1,\eta^2\text{-}C_2R')(\mu\text{-}\eta^1\text{-}C_2R)]$ [14]. Where R = R′ = Et, a β-H atom is transferred to the Os_3 core and the resulting (Me)(H)C=C–C≡C–Et ligand adopts a $\mu_3\text{-}\eta^2,\eta^2,\eta^1$ coordination mode. The reactions of $[M_3(CO)_9(\mu\text{-CO})(\mu_3\text{-}\eta^2\text{-}RC_2C_2R')]$ with $[Co_2(CO)_8]$ also illustrate the difference in reactivity between the Ru and Os analogues; for M = Ru, R = R′ = Ph, Ru–Ru and Co–Co bond cleavage occurs to generate $[Co_2Ru_3(\mu_5\text{-}\eta^2,\eta^2\text{-}PhC_2C_2Ph)]$ with a bow-tie metal core, whereas for M = Os, R = H, R′ = $SiMe_3$ a '$Co_2(CO)_6$' unit coordinates to the free C≡C bond in a $\mu\text{-}\eta^2$ manner [16–18].

We have re-investigated the reaction of MeC_2C_2Me with the activated triosmium cluster $[Os_3(CO)_{10}(NCMe)_2]$ at ambient temperature in order to identify the other products of the reaction, only $[Os_3(CO)_9(\mu\text{-CO})(\mu_3\text{-}\eta^2\text{-}MeC_2C_2Me)]$ (**1**) being isolated previously in 16% yield [13]. In addition, we have studied the reactions of some of these products and of the PhC_2C_2Ph analogue of **1** with $[Co_2(CO)_8]$ and Me_3NO–NCMe. The structures of four of the new compounds have been confirmed by single-crystal X-ray crystallography.

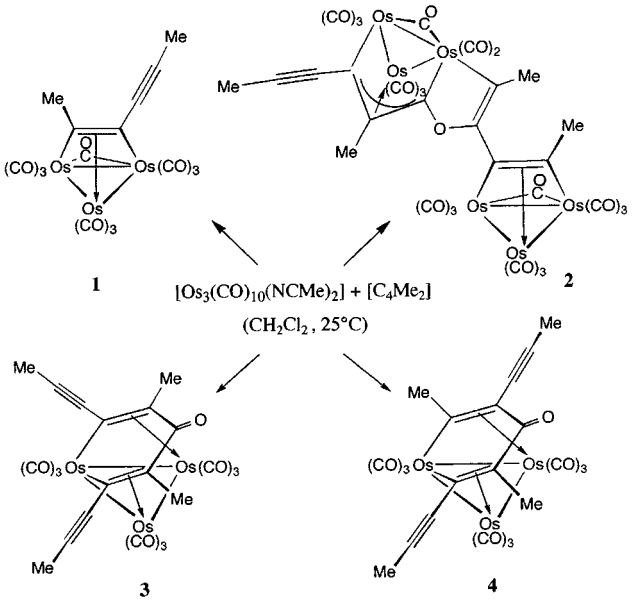

Scheme 1.

2. Results and discussion

2.1. Reaction of $[Os_3(CO)_{10}(NCMe)_2]$ with MeC_2C_2Me

The room temperature reaction of MeC_2C_2Me with $[Os_3(CO)_{10}(NCMe)_2]$ generates four products, the yields of which are dependent on the reaction stoichiometry. When the reaction is carried out in a 1:1 molar ratio of ligand to cluster reagent the known complex $[Os_3(CO)_9(\mu\text{-CO})(\mu_3\text{-}\eta^2\text{-}MeC_2C_2Me)]$ (**1**) is isolated as orange oily solid in 15% yield as reported previously [13,14]. Spectroscopic and mass spectrometric analysis of the other three products was consistent with the formulation $[Os_3(CO)_{10}(C_4Me_2)]_2$ for a dark orange solid **2**, isolated in 30% yield, and $[Os_3(CO)_{10}(MeC_2C_2Me)_2]$ for both the deep purple oily solid **3**, obtained in 35% yield and the rose coloured product **4** isolated in 5% yield (Scheme 1). Spectroscopic and analytical data for the new complexes are summarised in Table 1.

The IR spectrum of **2** exhibits a broad absorption at 1841 cm^{-1}, indicating the presence of a bridging carbonyl ligand, and a ν(C≡C) triple bond absorption is observed at 2108 cm^{-1}. ^{1}H- and ^{13}C-NMR spectroscopy revealed the presence of four chemically inequivalent methyl groups, indicating that the two diyne ligands and consequently the two triosmium units adopt different environments. The ^{13}C-NMR spectrum is poorly resolved but exhibits two approximately equal intensity resonances in the terminal carbonyl region, providing evidence for discrete cluster-localised carbonyl fluxionality. The negative ion FAB mass spectrum showed an m/z of 1830 that corresponds to the formulation minus one CO ligand. The molecular structure of $[Os_3(CO)_9(\mu\text{-CO})(\mu_3\text{-}\eta^2\text{:}\mu_3\text{-}\eta^1\text{:}\eta^1\text{:}\eta^3\text{-}MeC_2C_2MeOC_5Me_2)Os_3(\mu\text{-CO})(CO)_9]$ (**2**) has been determined by single-crystal X-ray diffraction (Fig. 1, Table 2) and is consistent with the IR and NMR spectral data.

One Os_3 unit is σ-bound to the hydrocarbon ligand through Os(4) and Os(5) and is coordinated in a π-allyl manner through C(14), C(15) and C(17) to Os(6). Os(4) is incorporated into a metallocycloether ring by two σ-interactions to C(20) and C(17). The ring oxygen atom, O(18), has single bond C–O distances of 1.36(2) and 1.40(2) Å, whereas the C(19)–C(20) distance of 1.36(2) Å is characteristic of a double bond. The second trisomium unit aside, the product is analogous to the clusters $[Os_3(\mu\text{-CO})(CO)_8(R_1C{=}C(R_2)OC{-}C(R_3){=}CR_4)]$

Table 1
Spectroscopic and microanalytical data for the new complexes **2**–**4**, **6**–**18**

	IR ν(cm^{-1}) (CH_2Cl_2)	^{1}H-NMR (δ, J/Hz)	^{13}C-NMR (δ)	Microanalysis (% C, H) [a]	Mass spectroscopy [a]
2	2108(w), 2094(m), 2065(vs), 2060(vs), 2054(sh), 2023(vs), 1998(m), 1841(w, br)	[b,c] 2.78 (s, 3H, C(16)H_3), 2.62 (s, 3H, C(24)H_3), 2.36 (s, 3H, C(21)H_3), 2.15 (s, 3H, C(11)H_3)	[b,d] 271.00 (s, 2C, μCO), 182.58 (s, 10C, 10CO),174.72 (s, 8C, 8CO), 71.93, 78.83 (2s, 2C, C^{alk}), 89.07, 97.62, 99.14 (3s, 3C, C^{allyl}), 115.00, 123.45 (2s, 2C, $C^{c=c}$), 42.10, 39.88, 30.15, 20.22 (4s, 4C, CH_3)	C 20.73 (20.67); H 0.8 (0.67)	1830 (1858)
3	2109(mw), 2080(s), 2055(s), 2023(vs), 2001(m), 1974(sh), 1621(w, br)	[b,c] 2.48 (s, 6H, C(117)/C(115)H_3), 2.27 (s, 6H, C(111)/C(101)H_3)	[b] 177.14 (s{br}, 9C, CO), 135.58 (s, 2C, $C^{c=c}$), 103.42 (s, 2C, C^{alk}), 102.47 (s, 2C, $C^{c=c}$), 85.29 (s, 2C, C^{alk}), 31.91, 27.39 (s, 2C, CH_3)	C 29.28 (29.54); H 1.08 (1.13)	1006 (1006)
4	2114(w), 2094(s), 2064(vs), 2053(vs), 2040(sh), 2025(s), 2010(sh), 1986(sh)	[b] 3.47 (s, 3H, Me), 2.47 (s, 3H, Me) 2.29 (s, 3H, Me), 2.02 (s, 3H, Me)	[b] 164.25 (s, 9C, 9CO), 59.35, 45.31, 29.71, 27.07 (4s, 4C, CH_3)	C 29.38 (29.54); H 1.16 (1.13)	1006 (1006)
6	2102(vw), 2081(s), 2063(vs), 2052(sh), 2021(s), 2004(sh), 1841(w, br)	[b] 2.86 (s, 3H, Me), 2.79 (s, 3H, Me)	[d]	C 21.60 (21.70); H 0.44 (0.49)	1215 (1215)
7	2100(vw), 2093(s), 2081(s), 2062(vs,br), 2017(vs, br), 2000(sh), 1830(m, br)	[b] 2.93 (s{br}, 3H, Me), 2.74 (s{br}, 3H, Me), 2.43 (s{br}, 3H, Me), 2.35 (s{br}, 3H, Me)	[b,d] 204.35 (s, 6C, 6CO), 173.89 (s, 10C, 10CO), 173.39 (s, 10C, 10CO), 53.42, 30.03, 28.10, 22.69 (4s, 4C, CH_3)		2116 (2144)
8	2116(w), 2096(m), 2082(s), 2062(s), 2055(vs), 2020(s), 2007(sh), 1979(m), 1604(w)	[b] 3.12 (s{br}, 3H, Me), 2.92 (s{br}, 3H, Me), 2.45 (s{br}, 3H, Me), 2.29 (s{br}, 3H, Me)	[b,d] 206.44 (s{br}, 6C, 6CO), 195.24 (s{br}, 9C, CO), 38.79, 33.14, 29.02, 26.31 (4s, 4C, CH_3)		1268 (1296)
9	2110(w), 2097(w), 2081(s), 2058(s), 2023(vs), 2006(s), 1978(sh), 1618(w, br)	[b,d]	[d]		1296 (1296)
10	2110(w), 2095(m), 2082(s), 2062(s), 2054(vs), 2027(s), 2009(sh), 1979(sh), 1624(w, br)		[d]		1296 (1296)
11	2103(m), 2084(s), 2066(vs), 2056(vs), 2029(m), 2006(m), 1840(w, br)	[b] 7.76–7.14 (m, 10H, Ph)	[b,d] 199.50 (s, 10C, 10CO), 176.83 (s, 6C, 6CO)	C 27.53 (28.50); H 0.87 (0.78)	1312 (1340)

Table 1 (*Continued*)

	IR ν(cm^{-1}) (CH_2Cl_2)	^{1}H-NMR (δ, J/Hz)	^{13}C-NMR (δ)	Microanalysis (% C, H) [a]	Mass spectroscopy [a]
12	2097(mw), 2080(m), 2071(sh), 2068(m), 2046(sh), 2044(vs), 2011(m), 2000(m), 1958(m)	[b] 2.81 (s, 3H, Me), 2.71 (s, 3H, Me), 2.08 (s, 3H, Me)			902 (943)
13	2097(m), 2080(m), 2069(s), 2054(vs), 2046(sh), 2044(vs), 2011(m), 2000(m),	[b] 7.85–6.98 (m, 10H, Ph), 2.29 (s, 3H, NCCH_3)			1030 (1071)
14, **15**	2094 (s), 2065(vs), 2038(vs), 2019(s), 2006(m), 1989(s)	[b] 6.92 (q, 1H, $^3J = 6.64$, CHPh^{maj}), 6.19 (q, 1H, $^3J = 6.64$,CHPh^{min}), 3.48 (s, 3H, Me^{min}), 3.32 (s, 3H, Me^{maj}), 2.38 (d, 3H, $^3J = 6.70$, Me^{min}), 2.15 (s, 3H, $^3J = 6.66$, Me^{maj}), −4.08 (s, 2H$^{maj+min}$, μ-OH)		C 20.28 (19.56); H 1.02 (0.86)	920 (920)
16	2096 (vs), 2069(vs), 2043(vs), 2024(vs), 2012(s), 1995(s), 1986(sh)	[b,c] 7.88–7.06 (m, 10H, Ph), 7.28 (s, 1H, CHPh), −3.80 (s, 1H, OH)	[b,c] 184.40, 179.77, 178.90, 175.17, 174.81, 173.34, 172.22, 171.63, 164.85 (9s, 9C, 9CO), 149.90, 142.72 (2s, 2C, C^{ipso}), 138.80, 137.17, 133.49 (3s, 3C, $C^{trienyl}$), 122.53 (s, 1C, C(H)Ph), 128.79, 128.53, 128.34, 128.01, 127.91, 127.61 (6s, 6C, Ph)	C 28.92 (28.73); H 0.98 (1.14)	1044 (1044)
17	2209(mw), 2098(m), 2069(vs), 2044(vs), 2007(vs), 1984(s), 1954(s), 1669(m)	[b] 2.44 (s, 3H, NCMe), 2.20 (s, 6H, Me), 2.17 (s, 6H, Me)	[b,d] 208.16 (s, 2C, CO), 181.04 (s, 6C, CO), 135.75, 119.64 (2s, 4C, $C^{c=c}$), 98.87, 85.39 (2s, 4C, C^{alk}), 20.04 (s, 1C, NCCH$_3$), 18.65, 5.02 (2s, 4C, CH$_3$)	C 28.76 (27.03); H 1.76 (1.47); N 1.95 (1.37)	979 (1021)
18	2110(w), 2077(vs), 2067(ms), 2041(vs), 2011(vs), 1979(m), 1939(m), 1624(w)	[b] 3.38 (s, 9H, NMe_3), 2.53 (s, 6H, Me), 2.23 (s, 6H, Me)	[b,d] 187.46 (s, 2C, CO), 178.03 (s, 6C, CO), 142.01, 102.83 (2s, 4C, $C^{c=c}$), 93.26, 86.40 (s, 2C, C^{alk}), 61.46 (s, 3C, N(CH$_3$)$_3$), 27.08, 4.81 (2s, 4C, CH$_3$)	C 26.80 (27.74); H 1.54 (2.00); N 0.85 (1.34)	979 (1038)

[a] Calculated values in parentheses.

[b] $CDCl_3$ sample solution.

[c] C(#)H_n indicates atom numbering scheme for relevant molecular structure.

[d] Poorly resolved or broad spectra preclude complete assignment.C^{alk}: denotes free alkyne moiety. C^{allyl}: denotes allyl functionality associated carbon atom. $C^{c=c}$: denotes alkene group associated carbon atom.

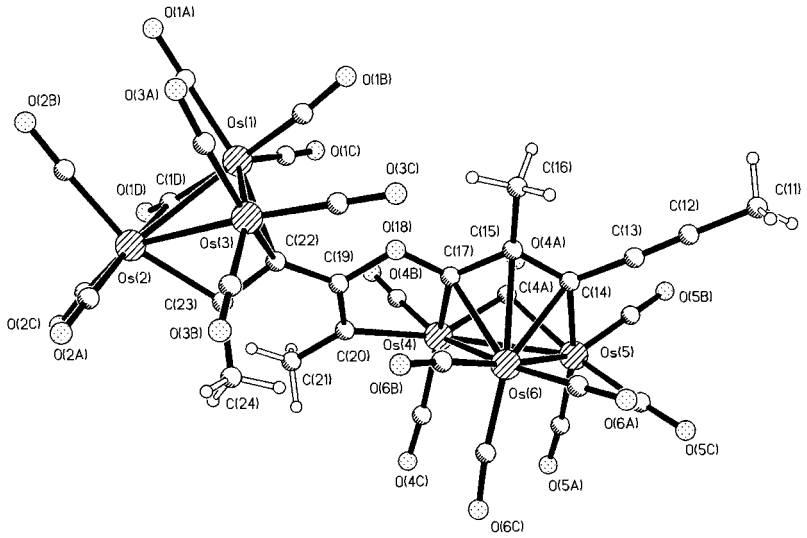

Fig. 1. Molecular structure of **2** showing the atom numbering scheme.

prepared by the reaction of $[Os_3(CO)_{10}(NCMe)_2]$ with the respective alkynes [6], the two alkyne groups being linked via the incorporation of a coordinated CO ligand. In the present case, one of the free triple bonds is sufficiently accessible sterically to permit the coordination of a further $Os_3(CO)_{10}$ unit in a typical μ_3-(η^2-$\|$) manner. In this coordination mode the linked diyne ligands donate a total of ten electrons, four to the μ_3-(η^2-$\|$) bound triosmium unit and six electrons to the other. Two carbonyl ligands bridge the Os(1), Os(2) and Os(4), Os(5) edges while the remaining 17 CO ligands are terminally bound and essentially linear.

The IR spectrum of **3** exhibits only ν(CO) signals corresponding to terminal CO ligands, but an absorption at 1619 cm^{-1} indicates the presence of an acyl C=O group and further weak ν(C≡C) absorption at 2112 cm^{-1} is observed. Only two distinct methyl resonances were observed in the ^{1}H-NMR spectrum of **3**, at 2.47 and 2.27 ppm, suggesting the presence of a mirror plane in the molecule. A single sharp resonance is observed at 184.06 ppm in the ^{13}C-NMR spectrum, indicative of carbonyl scrambling over the metal triangle. These data are consistent with the presence of a functionalised, osmacyclohexadienone ring, i.e. the formulation $[Os_3(CO)_9\{\mu_3$-η^4-$[(MeC_2)C_2(Me)]CO[(Me)C_2$-$(C_2Me)]\}]$ for **3**. The FAB mass spectrum exhibited a peak corresponding to the molecular ion. This has been confirmed by a single-crystal X-ray analysis (Fig. 2, Table 3) which demonstrates that the molecule does not have crystallographic mirror symmetry in the solid state. A similar structure has been proposed for $[Os_3(CO)_9\{[\mu_3$-η^1:η^1:η^2:η^2-$MeC_2(Me)]_2CO\}]$, which may be prepared by an analogous route [5], and a crystal structure determination has been performed for its $[P(OMe)_3]$ derivative [7]. In the structure of **3**, Os(2) has been incorporated into the carbocyclic ring by two σ-interactions from C(104) and C(108) and the ring is π-bound to Os(1) and Os(2) through C(107), C(108) and C(104), C(105) respectively, the cyclised ligand acting as a six electron donor. The pendant alkynes are essentially linear, as are the nine terminal carbonyl ligands. The C–C bonds that connect the pendant alkynes to the ring incorporated carbon atoms, C(108) and C(104), are only 0.03 Å longer than the alkyne and the ring incorporated carbon atoms. The bond lengths

Table 2
Selected bond lengths (Å) and angles (°) for complex **2**

Bond lengths			
Os(1)–Os(2)	2.862(2)	Os(6)–C(14)	2.29(2)
Os(2)–Os(3)	2.7544(12)	Os(6)–C(15)	2.33(2)
Os(1)–Os(3)	2.7614(13)	Os(6)–C(17)	2.28(2)
Os(4)–Os(5)	2.879(2)	C(11)–C(12)	1.45(3)
Os(5)–Os(6)	2.7787(14)	C(12)–C(13)	1.19(3)
Os(4)–Os(6)	2.8731(12)	C(13)–C(14)	1.46(2)
Os(1)–C(22)	2.18(2)	C(14)–C(15)	1.40(2)
Os(2)–C(23)	2.10(3)	C(15)–C(16)	1.53(2)
Os(3)–C(23)	2.30(2)	C(15)–C(17)	1.46(2)
Os(3)–C(22)	2.31(2)	C(17)–O(18)	1.36(2)
Os(4)–C(20)	2.11(2)	O(18)–C(19)	1.40(2)
Os(4)–C(17)	1.99(2)	C(19)–C(20)	1.36(2)
Os(5)–C(14)	2.14(2)	C(20)–C(21)	1.45(2)
Bond angles			
Os(1)–Os(2)–Os(3)	58.86(3)	Os(5)–C(4a)–O(4a)	131(2)
Os(2)–Os(1)–Os(3)	58.62(3)	Os(4)–C(17)–C(15)	127.7(13)
Os(1)–Os(3)–Os(2)	62.51(4)	Os(5)–C(14)–C(15)	127.3(14)
Os(4)–Os(5)–Os(6)	61.01(4)	C(11)–C(12)–C(13)	179(2)
Os(4)–Os(6)–Os(5)	61.21(4)	C(12)–C(13)–C(14)	174(2)
Os(5)–Os(4)–Os(6)	57.78(3)	C(14)–C(15)–C(16)	121(2)
Os(1)–C(1d)–O(1d)	153(2)	C(17)–C(15)–C(16)	123(2)
Os(2)–C(1d)–O(1d)	80.7(8)	C(17)–O(18)–C(19)	111.8(13)
Os(4)–C(20)–C(19)	111.8(12)	C(21)–C(20)–C(19)	124(2)
Os(4)–C(17)–C(18)	119.3(12)	C(20)–C(19)–C(22)	125(2)
Os(4)–C(4a)–O(4a)	144(2)	C(19)–C(22)–C(23)	127(2)

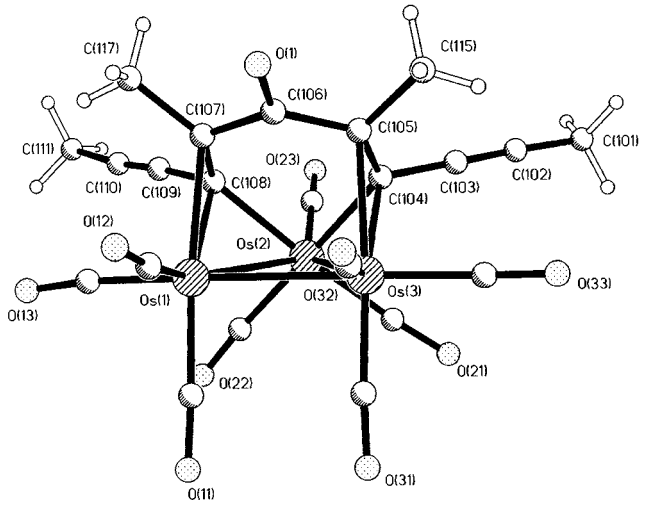

Fig. 2. Molecular structure of **3** showing the atom numbering scheme.

Table 3
Selected bond lengths (Å) and angles (°) for complex **3**

Bond lengths			
Os(1)–Os(2)	2.8184(9)	C(106)–O(1)	1.26(2)
Os(2)–Os(3)	2.8025(9)	C(106)–C(107)	1.50(2)
Os(1)–Os(3)	2.8607(11)	C(107)–C(108)	1.39(2)
Os(2)–C(104)	2.107(14)	C(104)–C(103)	1.42(4)
Os(2)–C(108)	2.11(8)	C(103)–C(102)	1.23(2)
Os(1)–C(107)	2.317(14)	C(102)–C(101)	1.41(3)
Os(1)–C(108)	2.22(2)	C(105)–C(115)	1.51(2)
Os(3)–C(104)	2.268(13)	C(108)–C(109)	1.45(2)
Os(3)–C(105)	2.324(14)	C(109)–C(110)	1.19(2)
C(104)–C(105)	1.45(2)	C(110)–C(111)	1.47(3)
C(105)–C(106)	1.45(2)	C(107)–C(117)	1.51(2)
Bond angles			
Os(1)–Os(2)–Os(3)	61.18(3)	C(103)–C(104)–C(105)	117.1(13)
Os(2)–Os(1)–Os(3)	59.13(2)	C(105)–C(106)–O(1)	118.6(14)
Os(1)–Os(3)–Os(2)	59.68(2)	C(107)–C(106)–O(1)	118.4(13)
Os(2)–C(108)–C(107)	126.5(11)	C(105)–C(106)–C(107)	122.8(12)
Os(2)–C(104)–C(105)	124.0(10)	C(106)–C(107)–C(108)	123.3(13)
C(104)–Os(2)–C(108)	85.6(5)	C(107)–C(108)–C(109)	116.9(13)
C(101)–C(102)–C(103)	178(2)	C(108)–C(109)–C(110)	176(2)
C(102)–C(103)–C(104)	175(2)	C(109)–C(110)–C(111)	174(2)

C(107)–C(108) and C(104)–C(105) are 1.39(2) and 1.45(2) Å respectively, exhibiting the characteristic lengthening observed when this type of olefinic-metal π interaction is present and the C(110)–C(109) and C(103)–C(102) bond lengths of 1.23(2), 1.19(2) Å are comparable to those in the free alkyne.

Spectroscopic data for **4** are consistent with it being a structural isomer $[Os_3(CO)_9\{\mu_3\text{-}\eta^4\text{-}[(MeC_2)C_2(Me)]\text{-}CO[(MeC_2)C_2(Me)]\}]$ of **3**, with the same molecular ion in the mass spectrum and the IR spectrum of **4** also showing the presence of a ring incorporated acyl functionality at 1614 cm^{-1}. Four discrete methyl signals are observed in the ^{1}H-NMR spectrum which indicates a loss of mirror symmetry, the positions of one pair of propynyl and methyl substitutents being reversed (Scheme 1).

The mechanisms for the formation of these clusters is unclear. When **1** is isolated in solution it shows no propensity to undergo the cyclisation reaction observed for **2**, nor does it react with a further equivalent of MeC_2C_2Me to produce **3** or **4**. When a dichloromethane solution of MeC_2C_2Me is added dropwise to a solution of $[Os_3(CO)_{10}(MeCN)_2]$ over the period of 1 h, the yield of **1** is maximised whereas, when MeC_2C_2Me is added quickly to a solution of $[Os_3(CO)_{10}(MeCN)_2]$, the yields of **2**, **3** and **4** are increased and the reaction conditions cannot be further altered so as to preclude the formation of any particular product. It is therefore proposed that **2** is formed via the reaction of MeC_2C_2Me (or **1**) with $[Os_3(CO)_{11}(MeCN)(MeC_2\text{-}C_2Me)]$, i.e. an intermediate that has an η^2-coordinated alkyne moiety and an acetonitrile ligand. No evidence for this, presumably short-lived, compound has been found, possibly due to the propensity of the diyne molecule to displace the second MeCN ligand. Similarly, **3** and **4** could be formed by the reaction of a free molecule of $[MeC_2C_2Me]$ with such an intermediate (Scheme 2).

2.2. Reactions of *1–5* with $[Co_2(CO)_8]$

Clusters **1**–**4** and $[Os_3(CO)_9(\mu\text{-}CO)(\mu_3\text{-}\eta^2\text{-}PhC_2C_2Ph)]$ (**5**) have been shown to be unreactive towards a second molecule of $[Os_3(CO)_{10}(NCMe)_2]$ because of the steric demands of the inclusion of a second triosmium unit [10]. To investigate the reactivities and steric constraints imposed on the pendant alkyne moieties by the adjacent triosmium units, clusters **1**–**5** were stirred with

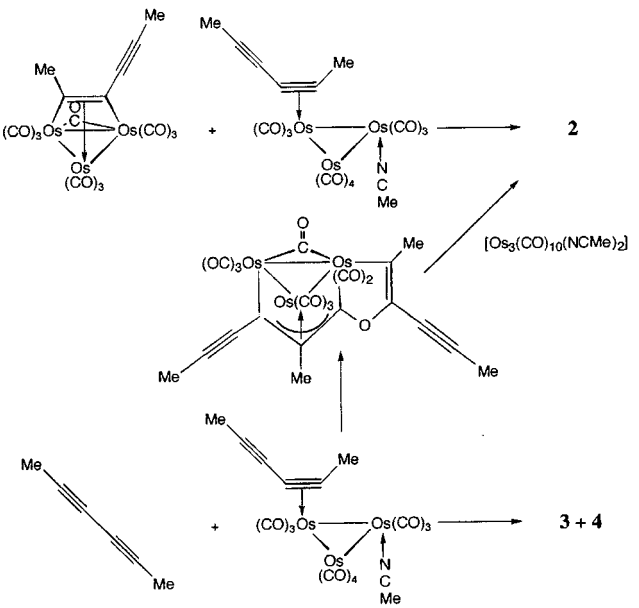

Scheme 2.

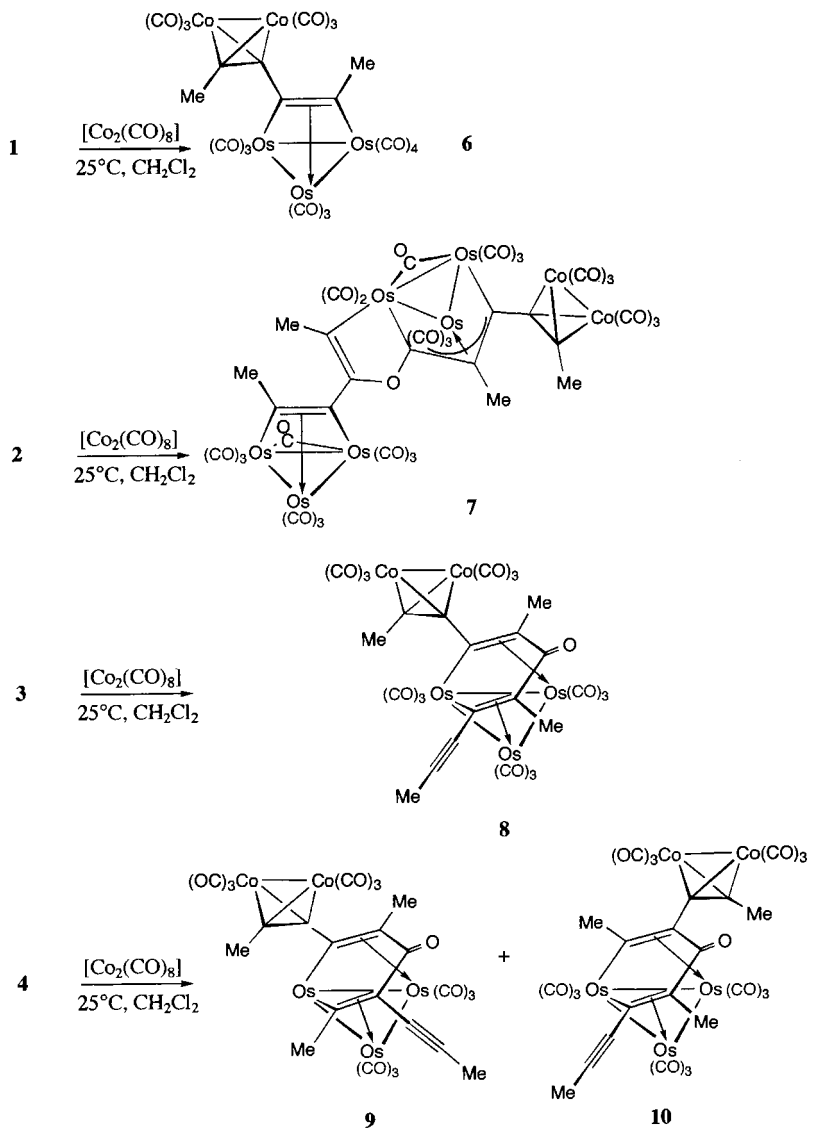

Scheme 3.

$[Co_2(CO)_8]$ that acts as the source of the less sterically demanding '$Co_2(CO)_6$' group.

The reaction of **1** with a slight excess of $[Co_2(CO)_8]$ results in the immediate generation of the olive green diyne-linked cluster $[Os_3(CO)_{10}\{\mu_3\text{-}\eta^2\text{:}\mu\text{-}\eta^2\text{-}MeC_2C_2Me\text{-}[Co_2(CO)_6]\}]$ (**6**) as the sole product (Scheme 3). The complex was characterised initially by spectroscopic and mass spectrometric techniques, the molecular ion being observed in the FAB mass spectrum, and the structure confirmed by a single-crystal X-ray analysis. The molecular structure of **6** (Fig. 3, Table 4) is similar to that of the known $HC_2C_2SiMe_3$ analogue [15].

In the molecular structure of **6** the osmium triangle is capped by one of the alkyne units {C(4)–C(5)} of the diyne. The diyne is a linked to the '$Co_2(CO)_6$' fragment through the C(2)–C(3) alkyne unit. The C(2)–C(3) distance is shorter than C(4)–C(5) as might be expected for the dimetal bridging alkyne as opposed to the trimetal bridging alkyne. The cluster shows no propensity to undergo oxidation in air but addition of an oxidising agent such as $[Fe(NO_3)_3]$ results in the facile loss of the dicobalt unit and the regeneration of the starting cluster **1**.

When slightly more than one molar equivalent of $[Co_2(CO)_8]$ is added to **2**, the linked cluster $[Os_3(\mu\text{-}CO)(CO)_9\{\mu_3\text{-}\eta^2\text{-};\mu_3\text{-}\eta^1\text{:}\eta^1\text{:}\eta^3\text{-};\mu\text{-}\eta^2\text{-}MeC_2C_2MeOC\text{-}(C_5Me_2)[Os_3(\mu\text{-}CO)(CO)_8][Co_2(CO)_6]\}$ (**7**) is isolated in near quantitative yield (Scheme 3). The '$Co_2(CO)_6$' unit is very labile and **7** decomposes quantitatively to **2** in a few hours unless stored under N_2 at -20 °C. Three discrete CO signals are observed in the ^{13}C-NMR spectrum, indicating the presence of localised dynamic behaviour over each of the cluster units. The loss of the carbon–carbon triple bond absorption in the IR spec-

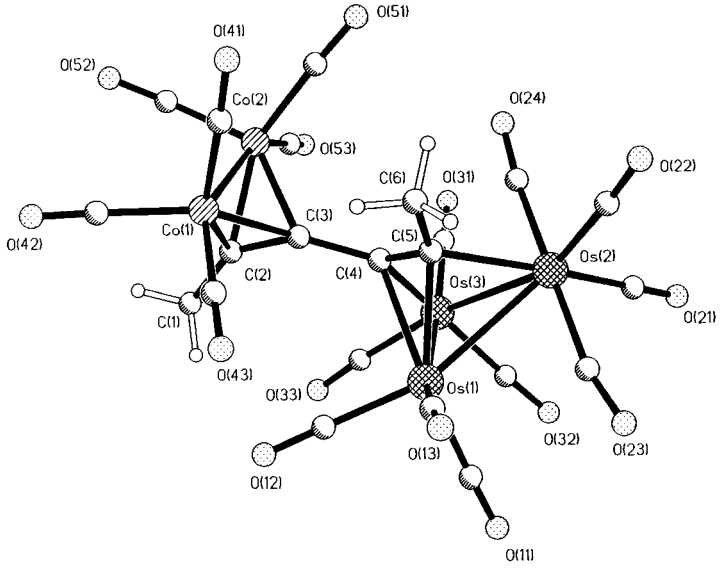

Fig. 3. Molecular structure of **6** showing the atom numbering scheme.

trum of **7** demonstrates that the dicobalt unit adds across the remaining C≡C bond. The addition of a '$Co_2(CO)_6$' is confirmed by the mass ion being observed at $m/z = 2116$, in the FAB mass spectrum, a value that corresponds to the molecular ion less one CO group.

The related reaction with **3** affords an air-unstable blue solid $[Os_3(CO)_9\{\mu_3\text{-}\eta^1\text{:}\eta^1\text{:}\eta^2\text{:}\eta^2\text{-;}\mu\text{-}\eta^2\text{-}\{(MeC_2)C_2(Me)\}_2CO[Co_2(CO)_6]\}]$ (**8**), which decomposed quantitatively to reform **3** unless the solid is stored at −20 °C under N_2. The ^{1}H-NMR spectrum of **8** indicates the presence of four discrete methyl resonances, two of these remaining in a similar region to those found for **3**, and two moving downfield to δ 2.92 and 3.12 ppm, reflecting the coordination of a single dicobalt unit. The ν(C≡C) absorption for the other alkyne is still observed in the IR spectrum. The FAB mass spectrum exhibited a molecular ion peak corresponding to the formulation less one CO ligand. Similarly, the reaction of **4** yields two navy blue isomers of $[Os_3(CO)_9\{\mu_3\text{-}\eta^1\text{:}\eta^1\text{:}\eta^2\text{:}\eta^2\text{-;}\mu\text{-}\eta^2\text{-}\{(MeC_2)C_2(Me)\}_2CO\}\text{-}Co_2(CO)_6]$ (**9**) and (**10**), which differ in which of the pendant alkyne moieties remains uncoordinated. Here the molecular ion is observed in the FAB mass spectrum. In the reactions of **3** and **4** there is no evidence for the formation of *bis* adducts and the *mono* adducts are themselves inherently unstable.

The reaction of $[Os_3(CO)_9(\mu\text{-}CO)(\mu_3\text{-}\eta^2\text{-}PhC_2C_2Ph)]$ (**5**), the PhC_2C_2Ph-substituted analogue of **1**, with $[Co_2(CO)_8]$ affords a single dark green product which has been identified spectroscopically as the phenyl analogue of **6**, i.e. $[Os_3(CO)_{10}\{\mu_3\text{-}\eta^2\text{:}\mu\text{-}\eta^2\text{-}PhC_2C_2Ph[Co_2(CO)_6]\}]$ (**11**). The mass spectrum shows the molecular ion peak less one CO ligand. Monitoring the reaction by IR spectroscopy shows that the reaction proceeds at a much slower rate than for **1**, taking several hours to reach completion. ^{13}C-NMR reveals two discrete CO resonances at 199.50 and 176.83 ppm, the latter being considerably more intense, indicating complete scrambling on each metal unit. The cluster is not stable in air and decomposes quantitatively to **5** over a period of hours. Previous studies had suggested that rather than producing **11** the diyne was simply transferred to the dicobalt unit [17].

2.3. Reaction of *1–5* with Me_3NO in the presence of MeCN

Clusters **1**–**5** were treated with one equivalent of trimethylamine-*N*-oxide (Me_3NO) in the presence of acetonitrile in an attempt to activate these clusters towards further substitution of donor ligands. The reac-

Table 4
Selected bond lengths (Å) and angles (°) for complex **6**

Bond lengths			
Os(1)–Os(2)	2.8646(13)	C(1)–C(2)	1.50(2)
Os(2)–Os(3)	2.8633(12)	C(2)–C(3)	1.36(2)
Os(1)–Os(3)	2.705(2)	Co(1)–Co(2)	2.459(3)
Os(2)–C(5)	2.196(10)	Co(1)–C(2)	1.959(11)
Os(3)–C(4)	2.151(11)	Co(1)–C(3)	2.030(11)
Os(1)–C(4)	2.322(11)	Co(2)–C(2)	1.972(11)
Os(1)–C(5)	2.187(11)	Co(2)–C(3)	1.984(11)
C(4)–C(5)	1.41(2)	C(5)–C(6)	1.51(6)
C(3)–C(4)	1.46(2)		
Bond angles			
Os(1)–Os(2)–Os(3)	56.36(3)	C(5)–C(4)–Os(3)	109.9(7)
Os(2)–Os(1)–Os(3)	61.79(3)	C(3)–C(2)–C(1)	146.0(11)
Os(1)–Os(3)–Os(2)	61.84(3)	C(4)–C(3)–C(2)	145.0(10)
Os(2)–C(5)–Os(1)	81.6(4)	C(5)–C(4)–C(3)	124.6(9)
Os(1)–C(4)–Os(3)	74.3(3)	C(6)–C(5)–C(4)	126.3(10)
Os(2)–C(5)–C(4)	107.9(7)		

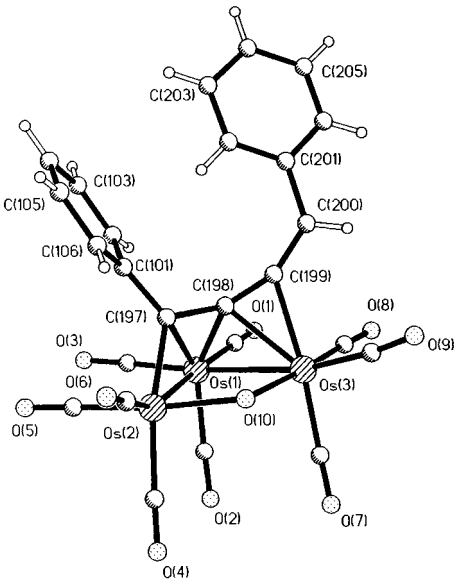

Fig. 4. Molecular structure of **16** showing the atom numbering scheme; the hydroxyl hydrogen is disordered over two positions and is not shown for clarity.

Table 5
Selected bond lengths (Å) and angles (°) for complex **16**

Bond lengths			
Os(1)–Os(2)	2.8218(14)	Os(3)–C(199)	2.21(2)
Os(1)–Os(3)	2.878(2)	Os(3)–C(198)	2.25(2)
Os(2)–O(10)	2.105(14)	C(197)–C(198)	1.43(3)
Os(3)–O(10)	2.114(14)	C(198)–C(199)	1.34(3)
Os(2)–C(197)	2.09(2)	C(199)–C(200)	1.34(3)
Os(1)–C(197)	2.29(2)	C(200)–C(201)	1.48(3)
Bond angles			
Os(2)–Os(1)–Os(3)	77.52(4)	C(101)–C(197)–C(198)	118(2)
Os(1)–Os(2)–O(10)	84.3(4)	C(197)–C(198)–C(199)	139(2)
Os(2)–O(10)–Os(3)	115.5(6)	C(198)–C(199)–C(200)	155(2)
Os(1)–Os(3)–O(10)	82.7(4)	C(199)–C(200)–C(201)	128(2)

tion of **1** leads to the generation of the yellow substitution product $[Os_3(CO)_9(NCMe)(\mu_3\text{-}\eta^2\text{-}MeC_2C_2Me)]$ (**12**) in 25% yield, as evidenced by three discrete methyl resonances in the ^{1}H-NMR spectrum; at δ 2.08, 2.71 and 2.81 ppm. The mass spectrum exhibits a peak corresponding to the molecular formulation less the NCMe ligand. The reaction of **5** produces the analogous yellow cluster $[Os_3(CO)_9(NCMe)(\mu_3\text{-}\eta^2\text{-}MeC_2C_2Me)]$ (**13**) in 20% yield. The vertex to which the MeCN ligand is coordinated is unknown.

In addition, the above reactions of **1** and **5** produce the high yielding products $[Os_3(CO)_9(\mu\text{-}OH)(\mu_3\text{-}\eta^1\text{:}\eta^2\text{:}\eta^2\text{-}MeC_3CHMe)]$ (**14**, **15**), identified spectroscopically as inseparable isomers, and $[Os_3(CO)_9(\mu\text{-}OH)(\mu_3\text{-}\eta^1\text{:}\eta^2\text{:}\eta^2\text{-}PhC_3CHPh)]$ (**16**), respectively, in which a water molecule replaces a CO or MeCN ligand, the water coming from the wet solvent mixture. The single-crystal X-ray structure of **16** has been determined and the molecular structure is illustrated in Fig. 4 (Table 5). The diyne ligand of the parent cluster has acquired a proton from a water molecule and the hydroxyl group, generated as a consequence of deprotonation, inserts into the Os(2)–Os(3) edge, forming a quadrilateral Os_3O core with the molecule having a cluster electron count of 50 electrons. The resulting 1,4-diphenyltriene-1-yl ligand donates five electrons to the cluster through a σ-bond to Os(2) and adjacent π interactions from C(197)–C(198), C(198)–C(199) to Os(1) and Os(3) respectively. The coordination of a 1,2,3-triene-1-yl ligand to an osmium or ruthenium cluster has not been observed previously, to our knowledge, although this coordination mode is similar to that of allenyl ligands in trinuclear 48 electron osmium and ruthenium clusters. The hydroxyl hydrogen atom was not directly located and is omitted from the structural diagram (Fig. 4). The three cumulated double bonds all exhibit bond lengths in keeping with the expected values and their directional alternation is evident. The terminal CO ligands are essentially linear.

The ^{1}H-NMR spectrum of the MeC_2C_2Me analogue reveals the presence of two isomeric products **14** and **15** in a 4:3 ratio. These exhibit a quartet resonance, at δ 6.92 ppm ($^3J = 6.64$ Hz) for the major and δ 6.19 ppm ($J = 6.64$ Hz) for the minor isomer, each relatively integrating for one proton. Two singlets (*δ 3.32 ppm, 3H, Me^{maj}, δ 3.48 ppm, 3H, Me^{min}) and two doublets (*δ 2.15 ppm, $^3J = 6.66$ Hz, 3H, Me^{maj}, δ 2.38 ppm, $^3J = 6.70$ Hz, 3H, Me^{min}) are also observed. A singlet resonance is also found at δ −4.08 ppm, having a combined integration of two single-proton intensities, one from a major and one from a minor isomer, which may be attributed to the OH proton. The signal shows some broadening with respect to the other signals and hydroxyl protons are notoriously highly dynamic and may be involved in hydrogen bonding or a fluxional process that could cause the signals for the two isomers to coincide. A satisfactory ^{13}C spectrum could not be obtained due to the poor solubility of the product in hydrocarbon solvents.

The two isomeric products observed in solution can be explained with reference to the structure of **16**. Whereas the Ph of the Ph(H)C=C group is directed away from the Os_3 core in the structure of **16**, the less sterically demanding methyl group could adopt the position adopted by the alkenic H in **16**. The barrier to rotation at 20 °C about the uncoordinated C=C bond is sufficient to allow the resolution of the alternative structural isomers **14** and **15** with the Me and H ligands in each of the two possible positions. The probable structures for **14** and **15** are shown in Fig. 5.

The ^{1}H-NMR spectrum of **16** indicates that only one structural form of this product exists in solution; the greater steric demands of the substituent phenyl groups on the diyne ligand prevent the formation of the alter-

native isomer. The well resolved ^{13}C-NMR spectrum indicates the occurrence of phenyl ring rotational fluxionality and a lack of carbonyl associated dynamic processes on the NMR timescale. The trienyl carbon backbone atoms, C(197)–C(198)–C(199), are observed at 137.17, 142.72 and 149.90 ppm, while the APT (attached proton transfer) spectrum revealed the C(200) resonance at 122.53 ppm.

The treatment of **12** with wet solvents yields a mixture of **14** and **15** quantitatively, the water molecule displacing the acetonitrile ligand. Although the water molecule may be derived solely from wet solvent, when great care is taken to exclude it, **14** and **15** continue to be produced; the water may be introduced with the Me_3NO reagent which is notoriously hygroscopic.

The reaction of Me_3NO–NCMe with **3** gives two air-stable products **17** (orange) and **18** (red) in which a CO group is substituted by NCMe or NMe_3 ligand, respectively, **3** being completely consumed. Both compounds exhibit similar spectroscopic properties to **3** and the mirror plane is retained, indicating that substitution has occurred at the metallacyclic Os vertex. This is the substitution position suggested for the MeCN ligand in $[Os_3(CO)_8(NCMe)\{[\mu_3\text{-}\eta^1\text{:}\eta^1\text{:}\eta^2\text{:}\eta^2\text{-}MeC_2(Me)]_2CO\}]$ and adopted by the phosphite ligand in $[Os_3(CO)_8\{P(OMe)_3\}\{[\mu_3\text{-}\eta^1\text{:}\eta^1\text{:}\eta^2\text{:}\eta^2\text{-}MeC_2(Me)]_2CO\}]$ [7]. The ^{1}H-NMR spectrum of **17** displays three resonances at δ 2.44, 2.20 and 2.17 ppm in the ratio of 2:1:2, whereas **18** displays signals at δ 3.38, 2.53 and 2.23 ppm integrating in the ratio of 3:2:2. The ^{13}C-NMR spectrum includes an intense signal at 61.46 ppm corresponding to the trimethylamine carbons (the NMe_3 being produced upon reduction of Me_3NO) [17]. The IR and ^{13}C spectra of **18** suggests that the presence of two semi-bridging CO ligands, which probably compensate for the poor σ-base character of the NMe_3 ligand. This effect is less marked in **17**, the two CO resonances being ca. 15 cm^{-1} higher than those in **18**. Despite this, both products are air stable and only decompose upon moderate heating. The related reaction with **2** produces a simple substitution product, the characterisation of which was not pursued further, whilst the activation of **4** with Me_3NO was not attempted due to its low yield.

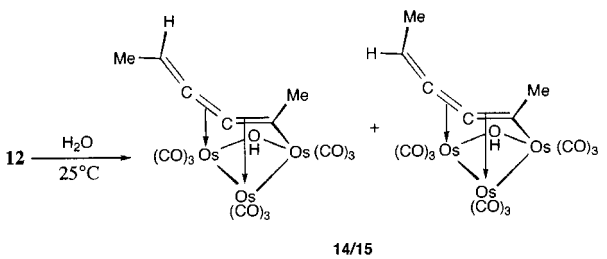

Fig. 5. Proposed isomeric structures of the products of the reaction of **12** with H_2O.

3. Experimental

3.1. General

All the reactions were performed using standard Schlenk techniques under an atmosphere of dry, oxygen-free nitrogen. Technical grade solvents were purified by standard procedures. $[Os_3(CO)_{10}(MeCN)_2]$ and $[Os_3(CO)_9(\mu\text{-}CO)(\mu_3\text{-}\eta^2\text{-}PhC_2C_2Ph)]$ [11] were prepared by the literature procedure and hexa-1,3-diyne, 1,4-diphenylbutadiyne and $[Co_2(CO)_8]$ were used as supplied. Infrared spectra were recorded as dichloromethane solutions in NaCl cell (0.5 mm path length) on a Perkin–Elmer 1710 Fourier transform spectrometer. Negative ion FAB mass spectra were recorded on an AE1/Kratos MS 50 spectrometer. NMR spectra were recorded on a Bruker WH 400 Fourier transform spectrometer in appropriate solvents. The chemical shifts were referenced to residual protons in $CDCl_3$ (7.25 ppm) or CD_2Cl_2 (5.33) for ^{1}H and to $CDCl_3$ (77.0 ppm) for ^{13}C. Spectroscopic data for all new compounds are given in Table 1.

3.2. Reaction of $[Os_3(CO)_{10}(NCMe)_2]$ with MeC_2C_2Me

A CH_2Cl_2 solution of MeC_2C_2Me (17 mg, 0.21 mmol) was added dropwise to a CH_2Cl_2 solution of $[Os_3(CO)_{10}(NCMe)_2]$ (200 mg, 0.21 mmol). This mixture was stirred under nitrogen for 18 h and subsequently worked up and separated on silica plates. The orange band, isolated from the top of the plate, was recovered as an oily solid and identified by spectroscopic methods as $[Os_3(CO)_9(\mu\text{-}CO)(\mu_3\text{-}\eta^2\text{-}MeC_2C_2Me)]$ (**1**) (15%). A second dark orange band was recovered from the just below **1** on the plates, and subsequently identified as $[Os_3(\mu\text{-}CO)(CO)_9(\mu_3\text{-}\eta^2\text{:}\mu_3\text{-}\eta^1\text{:}\eta^1\text{:}\eta^3\text{-}MeC_2C_2MeOC_5Me_2)[Os_3(\mu\text{-}CO)(CO)_8]]$ (**2**) (30%). This was successfully recrystallised by slow evaporation of a CH_2Cl_2–hexane solution at room temperature (r.t.). The third product, isolated as a deep purple oily solid from the bottom of the plate, was obtained in 35% yield and formulated as $[Os_3(CO)_9\{\mu_3\text{-}\eta^4[(MeC_2)C_2(Me)]CO[(Me)C_2(C_2Me)]\}]$ (**3**). The fourth, rose coloured band, recovered from the baseline of the silica plates was found to have the formulation $[Os_3(CO)_9\{\mu_3\text{-}\eta^4[(MeC_2)C_2(Me)]CO[(MeC_2)C_2(Me)]\}]$ (**4**) (5%).

3.3. Reaction of **1** with $[Co_2(CO)_8]$

A CH_2Cl_2 solution of **1** (30 mg, 0.0323 mmol) was stirred with a slight excess of $[Co_2(CO)_8]$ (12 mg, 0.0351 mmol) under an atmosphere of nitrogen at r.t. After 18 h the solvent was removed under reduced pressure, leading to the isolation of a dark green product. Separation of the crude product on silica plates led to the recovery of olive-green $[Os_3(CO)_{10}\{\mu_3\text{-}\eta^2\text{:}\mu\text{-}\eta^2\text{-}MeC_2C_2\text{-}$

$Me[Co_2(CO)_6]\}]$ (**6**), in 55% yield, and a small amount of insoluble cobalt decomposition product. Treatment of a CH_2Cl_2 solution of **6** with a molar equivalent of $[Fe(NO_3)_3]$ resulted in the quantitative recovery of **1**.

3.4. Reaction of **2** with $[Co_2(CO)_8]$

A CH_2Cl_2 solution of **2** (30 mg, 0.0161 mmol) was stirred at 20 °C with a slightly more than 1 molar equivalent of $[Co_2(CO)_8]$ (5 mg, 0.0351 mmol) under an atmosphere of N_2. After 4 h the solvent was removed under reduced pressure, leading to the isolation of a dark brown product. Separation of the crude product on silica plates led to the recovery of brown $[Os_3(\mu\text{-}CO)(CO)_9\{\mu_3\text{-}\eta^2\text{-}:\mu_3\text{-}\eta^1\text{:}\eta^1\text{:}\eta^3\text{-}:\mu\text{-}\eta^2\text{-}(MeC_2C_2MeOC_5Me_2)\}][Os_3(\mu\text{-}CO)(CO)_8][Co_2(CO)_6]$ (**7**) in 80% yield, and a small amount of insoluble cobalt decomposition product. Treatment of a CH_2Cl_2 solution of **7** with a molar equivalent of $[Fe(NO_3)_3]$ results in the quantitative recovery of **2**.

3.5. Reaction of **3** with $[Co_2(CO)_8]$

The r.t. reaction of $[Co_2(CO)_8]$ (18 mg, 0.051 mmol) with **3** (50 mg, 0.0496 mmol) results in the production of a blue CH_2Cl_2 (35 cm^3) solution after 18 h. A N_2 purged alumina column was set up and chromatography of the blue band (CH_2Cl_2–hexane, 1:3 eluent) under a slight pressure of nitrogen resulted in the elution of a navy blue product $[Os_3(CO)_9\{\mu_3\text{-}\eta^1\text{:}\eta^1\text{:}\eta^2\text{:}\eta^2\text{-};\mu\text{-}\eta^2\text{-}\{(MeC_2)C_2(Me)\}_2CO[Co_2(CO)_6]\}]$ (**8**), in 40% yield, which requires storage under a N_2 atmosphere (exclusion of O_2) at −20 °C in order to prevent oxidation of the dicobalt unit and quantitative decomposition to **3**.

3.6. Reaction of **4** with $[Co_2(CO)_8]$

The reaction of $[Co_2(CO)_8]$ (18 mg, 0.051 mmol) with **4** (50 mg, 0.0496 mmol) at 20 °C results in the production of a blue solution. The reaction was allowed to proceed for 12 h and the solvent was removed under reduced pressure. Oxygen was excluded wherever possible and subsequent TLC on silica afforded two navy-blue products $[Os_3(CO)_9\{\mu_3\text{-}\eta^1\text{:}\eta^1\text{:}\eta^2\text{:}\eta^2\text{-};\mu\text{-}\eta^2\text{-}\{(MeC_2)C_2(Me)\}_2CO[Co_2(CO)_6]\}]$ (**9**) (40%) and (**10**) (40%), recovered from the middle of the plates. These require storage under a N_2 atmosphere at −20 °C in order to prevent oxidation of the dicobalt unit and quantitative decomposition to **4**.

3.7. Reaction of **5** with $[Co_2(CO)_8]$

A CH_2Cl_2 (20 cm^3) solution of **5** (30 mg, 0.0284 mmol) was treated with a CH_2Cl_2 (10 cm^3) solution of $[Co_2(CO)_8]$ (9.7 mg, 0.0284 mmol) at r.t., producing a dark green solution. Subsequent TLC (hexane–CH_2Cl_2, 3:1) affords a single dark green product $[Os_3(CO)_{10}\{\mu_3\text{-}\eta^2\text{:}\mu\text{-}\eta^2\text{-}PhC_2C_2Ph[Co_2(CO)_6]\}]$ (**11**) (high R_f), in 65% yield, and a small amount of cobalt decomposition material, located on the baseline. Removal of solvent from the recovered green solution affords a green solid that was recrystallised from dichloromethane at −20 °C, as dark green blocks.

3.8. Reaction of **1** with Me_3NO in MeCN

A wet, mixed acetonitrile–CH_2Cl_2 solution (25:25 cm^3) of **1** (60 mg, 0.0645 mmol) was treated dropwise with an acetonitrile solution (5 cm^3) of Me_3NO (5.5 mg, 0.066 mmol). Stirring for 30 min at r.t. resulted in the orange solution turning yellow. Continued stirring for 18 h was followed by solvent removal and TLC on thin silica plates. An orange product $[Os_3(CO)_9(NCMe)(\mu_3\text{-}\eta^2\text{-}MeC_2C_2Me)]$ (**12**) (25%) and a yellow product. $[Os_3(CO)_9(\mu\text{-}OH)(\mu_3\text{-}\eta^1\text{:}\eta^2\text{:}\eta^2\text{-}MeC_3CHMe)]$ (**14**, **15**) (65%, high R_f) were isolated.

3.9. Reaction of **2** with Me_3NO in MeCN

Cluster **2** (50 mg, 0.0268 mmol) was dissolved in CH_2Cl_2 (15 cm^3) and treated with one equivalent of Me_3NO (2.0 mg, 0.0270 mmol) in acetonitrile (5 cm^3) dropwise over 20 min. A colour change from orange to yellow was observed and the solution continued to be stirred for 18 h at 20 °C. Upon either solvent removal, or standing in air, the compound becomes brown in colour and any attempt to purify the mixture by chromatographic methods results in the formation of a brown insoluble baseline that resists removal from the plates.

3.10. Reaction of **3** with Me_3NO in MeCN

Cluster **3** (70 mg, 0.069 mmol) was dissolved in CH_2Cl_2 (25 cm^3) and treated with a molar equivalent of Me_3NO (5.35 mg, 0.070 mmol) acetonitrile solution (5 cm^3), added dropwise. The solution was stirred for 20 min, after which spot TLC showed that **3** is completely consumed. Subsequent TLC affords an orange (high R_f) and red band (low R_f) in approximately equal yields. Subsequent solvent removal under reduced pressure yielded two products $[Os_3(CO)_8(NCMe)(\mu_3\text{-}\eta^1\text{:}\eta^1\text{:}\eta^2\text{:}\eta^2\text{-}\{(MeC_2)C_2(Me)\}_2CO)]$ (**17**) and $[Os_3(CO)_8(NMe_3)(\mu_3\text{-}\eta^1\text{:}\eta^1\text{:}\eta^2\text{:}\eta^2\text{-}\{(MeC_2)C_2(Me)\}_2CO)]$ (**18**). **18** was recrystallised at −20 °C from a CH_2Cl_2 solution as large purple–red crystals.

3.11. Reaction of **5** with Me_3NO in MeCN

A wet acetonitrile solution of **5** (50 mg, 0.047 mmol) was treated dropwise with a molar equivalent solution

Table 6
Crystallographic data and structure refinement parameters for **2**, **3**, **6** and **16**

	2	**3**	**6**	**16**
Molecular formula	$C_{32}H_{12}O_{20}Os_6$	$C_{22}H_{12}O_{10}Os_3$	$C_{22}H_6Co_2O_{16}Os_3$	$C_{25}H_{12}O_{10}Os_3$
M	1857.62	1006.92	1214.73	1042.95
Crystal system	monoclinic	orthorhombic	triclinic	monoclinic
Unit cell dimensions				
a (Å)	38.82(2)	9.749(2)	9.166(4)	12.115(4)
b (Å)	9.106(2)	12.309(2)	10.698(6)	16.479(3)
c (Å)	28.32(2)	21.252(6)	16.368(8)	13.254(2)
α (°)	90	90	86.24(4)	90
β (°)	127.32(4)	90	88.63(3)	98.95(2)
γ (°)	90	90	65.08(3)	90
U (Å)^3	7963(8)	2550.2(10)	1454.0(13)	2613.9(11)
Space group	$C2/c$	$P2_12_12_1$	$P\bar{1}$	$P2_1/n$
Z	8	4	2	4
D_c (Mg m^{-3})	3.099	2.623	2.774	2.650
Crystal size (mm)	$0.15\times0.10\times0.10$	$0.34\times0.28\times0.20$	$0.30\times0.27\times0.08$	$0.20\times0.15\times0.10$
Crystal habit	Orange–red block	Black block	Dark red plate	Yellow block
$F(000)$	6560	1808	1096	1880
μ (mm^{-1})	19.15	14.96	14.25	14.60
Maximum, minimum relative transmission	0.417, 0.183	0.351, 0.123	0.623, 0.073	1.00, 0.588
Data collection range (°)	$2.7<\theta<50$	$7.0<2\theta<45$	$7.0<2\theta<45$	$5.5<2\theta<45$
Index ranges	$0\le h\le46$	$-10\le h\le10$	$-9\le h\le9$	$0\le h\le13$
	$-10\le k\le10$	$-13\le k\le13$	$-11\le k\le11$	$0\le k\le17$
	$-33\le l\le26$	$-22\le l\le22$	$-17\le l\le\le17$	$-14\le l\le\le14$
Reflections measured	11625	3872	5018	3758
Independent reflections	6825 ($R_{int}=0.094$)	3328 ($R_{int}=0.030$)	3669 ($R_{int}=0.022$)	3404 ($R_{int}=0.064$)
Parameters	264	160	390	218
wR_2(all data) [a]	0.1546	0.0772	0.1054	0.1320
x, y [a]	0.0650, 124.0	0.0382, 27.50	0.0762, 3.03	0.0358, 12.89
R_1 [$I>2\sigma(I)$] [a]	0.0616	0.0325	0.0373	0.0475
Observed reflections	5505	3099	3335	2062
Goodness-of-fit on F^2 (all data) [a]	1.052	1.043	1.108	1.034
Maximum shift (σ)	0.001	0.001	0.001	0.001
Peak, hole in final difference map (e Å^{-3})	2.57, −3.45	1.21, −1.16	1.89, −2.06	1.74, −1.13
Extinction coefficient	0.00024(2)			
Absolute structure parameter		0.02(3)		

Data in common: graphite-monochromated Mo–K_α radiation, $\lambda=0.71073$ Å, $T=293(2)$ K.

[a] $R_1=\Sigma||F_o|-|F_c||/\Sigma|F_o|$. $wR_2=[\Sigma w(F_o^2-F_c^2)^2/\Sigma wF_o^4]^{1/2}$, $w=1/[\sigma^2(F_o)^2+(xP)^2+yP]$, $P=(F_o^2+2F_c^2)/3$, where x and y are constants adjusted by the program; goodness-of-fit $=[\Sigma[w(F_o^2-F_c^2)^2]/(n-p)]^{1/2}$ where n is the number of reflections and p the number of parameters.

of Me_3NO (3.6 mg, 0.047 mmol). The solution was stirred for 2 h, followed by removal of solvent at reduced pressure. TLC afforded two yellow products $[Os_3(CO)_9(NCMe)(\mu_3\text{-}\eta^2\text{-}PhC_2C_2Ph)]$ (**13**) (20%) and $[Os_3(CO)_9(\mu\text{-}OH)(\mu_3\text{-}\eta^1\text{:}\eta^2\text{-}PhC_3CHPh)]$ (**16**) (60%).

3.12. Crystal structure determination of *2*, *3*, *6* and *16*

Data were collected for **3** and **6** by the ω/θ scan method on a Stoe four-circle diffractometer and for **16** by the $\omega/2\theta$ method on a Rigaku AFC5R four-circle diffractometer. Three standard reflections measured at hourly intervals showed no significant variation in intensity. Cell parameters were obtained by least-squares refinement on diffractometer angles from 25 centred reflections ($20<2\theta<25°$). Semi-empirical absorption correction based on ψ-scan data were applied.

Data for **2** were collected on a Rigaku R-Axis IIc Imaging Plate (using $60\times3°$ oscillation frames) and processed using the TEXSAN package with a semi-empirical absorption correction based on symmetry-equivalent reflections being applied [19]. Cell parameters were obtained by least-squares refinement on diffractometer angles from 25 centred reflections ($30<2\theta<40°$) collected on a Rigaku AFC7R four-circle instrument.

The structures were solved by direct methods (heavy atom positions) and subsequent Fourier difference syntheses (SHELXTL PLUS [20]) and refined anisotropically on all non-H atoms (**6**), Os and O atoms (**16**) or heavy atoms alone (**2**, **3**) by full-matrix least-squares on F^2 (SHELXL 93 [21]). Hydrogen atoms were placed in idealised positions and refined using a riding model or as rigid methyl groups. The hydroxyl H in **16** could not be located and was modelled with half occupancy in both

tetrahedral positions. In the final cycles of refinement, weighting schemes were introduced which produced a flat analyses of variance. Crystal data and refinement details are given in Table 6.

4. Supplementary material

Crystallographic data (excluding structure factors) for the structures **2**, **3**, **6** and **16** have been deposited with the Cambridge Crystallographic Data Centre, CCDC nos. 160608, 160609, 160610 and 160611, respectively. Copies of this information may be obtained free of charge from The Director, CCDC, 12 Union Road, Cambridge CB2 1EZ, UK (Fax: +44-1223-336033; e-mail: deposit@ccdc.cam.ac.uk or www: http://www.ccdc.cam.ac.uk).

Acknowledgements

We thank the E.P.S.R.C. (L.P.C., G.P.S.) and the CCDC (G.P.S.) for financial support. We are also grateful to the European Community, INTAS grant no. 97-31999, for support for this project.

References

[1] C. Elschenbroich, A. Salzer, Organometallics, A Concise Introduction, VCH, Weinheim, 2nd edn., 1992.
[2] P.R. Raithby, M.J. Rosales, Adv. Inorg. Chem. Radiochem. 29 (1985) 169. E. Sappa, A. Tiripicchio, P. Braunstein, Chem. Rev. 83 (1983) 203.
[3] A.J. Deeming, S. Hasso, M. Underhill, J. Chem. Soc. Dalton Trans. (1975) 1614.
[4] B.F.G. Johnson, J. Lewis, K.T. Schorpp, J. Organomet. Chem. 91 (1975) C13. C.T. Sear, Jr., F.G.A. Stone, J. Organomet. Chem. 11 (1968) 644. G. Cetini, O. Gambino, E. Sappa, M. Valle, J. Organomet. Chem. 17 (1969) 437. E. Sappa, G. Cetini, O. Gambino, M. Valle, J. Organomet. Chem. 20 (1969) 195. G. Ferraris, G.A. Vaglio, O. Gambino, M. Valle, G. Cetini, J. Chem. Soc. Dalton Trans. (1972) 1998. G. Ferraris, G. Gervasio, J.Chem. Soc. Dalton Trans. (1973) 1933. G. Ferraris, G. Gervasio, J. Chem. Soc. Dalton Trans. (1974) 1813. A.A. Koridze, N.M. Astakhova, F.M. Dolgushin, A.I. Yanovsky, Y.T. Strutchkov, P.V. Petrovskii, Organometallics 14 (1995) 2167.
[5] W.G. Jackson, B.F.G. Johnson, J.W. Kelland, J. Lewis, K.T. Schorpp, J. Organomet. Chem. 88 (1975) C17.
[6] G. Gervasio, J. Chem. Soc. Chem. Commun. (1976) 25. V.V. Krivykh, O.A. Kizas, E.V. Vorontsov, F.M. Dolgushin, A.I. Yanovsky, Yu.T. Struchkov, A.A. Koridze, J. Organomet. Chem. 508 (1996) 39. S. Aime, G. Gervasio, L. Milone, E. Sappa, M. Franchini-Angela, Inorg. Chim. Acta 27 (1978) 145. S.L. Ingham, B.F.G. Johnson, P.R. Raithby, K.J. Taylor, L.J. Yellowlees, J. Chem. Soc. Dalton Trans. (1996) 3521.
[7] B.F.G. Johnson, R. Khattar, J. Lewis, P.R. Raithby, D.N. Smit, J. Chem. Soc. Dalton Trans. (1988) 1421.
[8] M.I. Bruce, Chem. Rev. 91 (1991) 197. S. Lotz, P.H. van Rooyen, R. Meyer, Adv. Organomet. Chem. 37 (1995) 219.
[9] M.I. Bruce, B.W. Skelton, A.H. White, N.N. Zaitseva, J. Chem. Soc. Dalton Trans. (1996) 3151. R.D. Adams, U.H.F. Bunz, W. Fu, G. Roidl, 578 (1999) 55.
[10] J.F. Corrigan, S. Doherty, N.J. Taylor, A.J. Carty, Organometallics 11 (1992) 3160.
[11] J.F. Corrigan, N.J. Taylor, A.J. Carty, Organometallics 13 (1994) 3378.
[12] L.P. Clarke, J.E. Davies, P.R. Raithby, G.P. Shields, J. Chem. Soc. Dalton Trans. (2000) 4527.
[13] P.J. Low, K.A. Udachin, G.D. Enright, A.J. Carty, J. Organomet. Chem. 578 (1999) 103.
[14] A.J. Deeming, M.S.B. Felix, P.A. Bates, M.B. Hursthouse, J. Chem. Soc. Chem. Commun. (1987) 461. A.J. Deeming, M.S.B. Felix, D. Nuel, Inorg. Chim. Acta 213 (1993) 3.
[15] M.I. Bruce, B.W. Skelton, A.H. White, N.N. Zaitseva, Aust. J. Chem. 49 (1996) 155.
[16] M.I. Bruce, N.N. Zaitseva, B.W. Skelton, A.H. White, Polyhedron 14 (1995) 2647.
[17] M.I. Bruce, P.J. Low, A. Werth, B.W. Skelton, A.H. White, J. Chem. Soc. Dalton Trans. (1996) 1551.
[18] L.P. Clarke, P.R. Raithby, G.P. Shields, Polyhedron 16 (1997) 3775.
[19] TEXSAN, Version 1.7-1, Molecular Structure Corporation, The Woodlands, TX, 1985, 1992, 1995. A.C.T. North, D.C. Phillips, F.S. Mathews, Acta Crystallogr. Sect. A 24 (1968) 351.
[20] SHELXTL PLUS, PC Release 4.0, Siemens Analytical X-Ray Instruments Inc., Madison, WI, 1990.
[21] U. Klabunde, Inorg. Synth. 15 (1974) 82.